Multiple Beam Two-Plasmon Decay: Linear Threshold to Nonlinear Saturation in Three Dimensions

J. Zhang, J. F. Myatt, R. W. Short, A. V. Maximov, H. X. Vu, D. F. DuBois, and D. A. Russell

Phys. Rev. Lett. **113**, 105001 — Published 2 September 2014

DOI: 10.1103/PhysRevLett.113.105001

Multiple beam two-plasmon decay: linear threshold to nonlinear saturation in three dimensions

J. Zhang,* J. F. Myatt, and A. V. Maximov

Laboratory for Laser Energetics, University of Rochester,

250 East River Road, Rochester NY 14623-1299 and

Department of Mechanical Engineering,

University of Rochester, Rochester, NY 14627

H. X. Vu

Electrical and Computer Engineering Department,

University of California, San Diego,

9500 Gilman Drive, La Jolla, CA 92093-0407

D. F. DuBois† and D. A. Russell

Lodestar Research Corporation, 2400 Central Avenue, P-5, Boulder, Colorado 80301

R. W. Short

Laboratory for Laser Energetics, University of Rochester,

250 East River Road, Rochester NY 14623-1299

Abstract

The linear stability of multiple coherent laser beams with respect to two-plasmon–decay instability in an inhomogeneous plasma in three dimensions has been determined. Cooperation between beams leads to absolute instability of long-wavelength decays, while shorter-wavelength shared waves are shown to saturate convectively. The multibeam, absolutely unstable form has the lowest threshold for most cases considered. Nonlinear calculations using a three-dimensional extended Zakharov model show that Langmuir turbulence created by the absolute instability modifies the convective saturation of the shorter-wavelength modes, which are seen to dominate at late times.

The parametric resonance of oscillators or waves is an effect that exists in areas of physics as diverse as geophysical fluid dynamics and galactic dynamics. Instabilities caused by the parametric excitation of waves in plasmas resulting from the presence of large-amplitude electromagnetic waves are of immediate concern to inertial confinement fusion (ICF) [1, 2], high-energy-density physics (HEDP), [3] and ionospheric modification experiments [4]. Most theoretical and numerical works to date have assumed that instability is driven by a single electromagnetic (EM) pump wave, despite the fact that almost all ICF and HEDP experiments overlap many beams. Recent indirect-drive experiments on the National Ignition Facility (NIF) (where 96 beams overlap near each of the two laser entrance holes of a plasma filled hohlraum) are examples that highlight the importance of cooperative, multiple-beam parametric instability. In these experiments a multiple-beam parametric instability known as cross-beam energy transfer (CBET) was shown to have a dramatic effect on implosion symmetry and target performance [5, 6]. In direct-drive ICF, where the fusion target is directly irradiated by many overlapping laser beams, two-plasmon decay (TPD) can occur. This problem has been studied for 40+ years, but there has been a strong resurgence of interest because of ignition-scale experiments on the NIF. TPD is important because it can generate hot electrons, which represent a preheat risk to the target [7]. TPD is a three-wave decay instability in which an EM wave of frequency ω_0 and wave vector $\vec{k}_0$ decays into two electrostatic Langmuir waves (LW's), satisfying the resonance conditions $\omega_0 = \omega + \omega'$ and $\vec{k}_0 = \vec{k} + \vec{k}'$, where ω, ω' and $\vec{k}$, $\vec{k}'$ are the frequencies and wave vectors of the decay LW's, respectively. This instability can occur in the coronal plasma at electron densities close to the quarter-critical density $n_c/4$, where $n_c[= m_e\omega_0^2/(4\pi e^2)]$ is the electron density at which EM waves are reflected. Here, e and m_e are the electron charge and mass, respectively.

A linear three-dimensional (3-D) numerical stability analysis of TPD in an inhomogeneous plasma driven by multiple laser beams is presented. This is followed by an investigation of the subsequent nonlinear evolution, where nonlinearity enters by the coupling of the LW's to low-frequency density perturbations. This model was in part motivated by a favorable comparison of the results with more-detailed, fully kinetic calculations in regimes where they can be compared (i.e., in two spatial dimensions) [8]. The results have completely revised our understanding of this multiple beam parametric instability. The existence of two forms of cooperative multiple-beam TPD instability is demonstrated. One form shares short-wavelength, high-group-velocity, cooperative (or common) LW's that convectively saturate

(i.e., the waves undergo a finite spatial amplification) [9], while the other is associated with shared long-wavelength, small-group-velocity LW's and is absolutely unstable (i.e., the waves grow in time). The identification of an absolutely unstable cooperative mode of instability is a new discovery. Furthermore, it is shown to have the lowest threshold in most cases. The presence of absolute instability with a low threshold renders the TPD an inherently nonlinear problem, the evolution of which is essentially different in three dimensions (all previous calculations were performed in 2-D).

The linear stability of multibeam TPD can be investigated by solving a linearized equation for the envelope of the electrostatic field [10, 11]:

$$\nabla \cdot \left[2i\omega_{\rm pe}(D_t + \nu_{\rm e}\circ) + 3v_{\rm e}^2\nabla^2 - \omega_{\rm pe}^2\delta N/n_0\right]\vec{E}_1 = \sum_{i=1}^{N} \frac{e}{4m_{\rm e}}\nabla \cdot [\nabla(\vec{E}_{0,\rm i}\cdot\vec{E}_1^*) - \vec{E}_{0,\rm i}\nabla\cdot\vec{E}_1^*]e^{-i\Omega_i t} + S_{\rm E}. \quad (1)$$

The quantity $\vec{E}_1$ is the complex temporal envelope of the real electrostatic field $\vec{E} = 1/2[\vec{E}_1(\vec{x},t)\exp(-i\omega_{\rm pe}t) + \text{c.c.}]$, where enveloping is carried out at the plasma frequency $\omega_{\rm pe} = (4\pi n_0 e^2/m_{\rm e})^{1/2}$ evaluated at the density $n_0 = 0.23\,n_{\rm c}$ for numerical convenience. In Eq. (1), $D_t \equiv (\partial_t + \vec{u}_0\cdot\nabla)$ is the convective derivative for a plasma with the flow velocity $\vec{u}_0$ (Plasma flow is a subdominant effect giving rise to a 10% to 15% increase in absolute threshold for a Mach-1 flow. For simplicity we assume $\vec{u}_0 = 0$). In the absence of EM pump waves, the free solutions to Eq. (1) are LW's that propagate in a density profile whose deviation from n_0 is given by δN ($\delta N \ll n_0$). [It has been assumed that the inhomogeneity is linear ($\delta N = n_0\,x/L_{\rm n}$) and the direction of its gradient defines the x axis.] LW's of wave number k have the group velocity $V_{\rm g} = 3kv_{\rm e}^2/\omega_{\rm pe}$, where $v_{\rm e} = \sqrt{T_{\rm e}/m_{\rm e}}$ is the electron thermal velocity, and their amplitudes damp at the rate $\nu_e = \nu_{\rm coll} + \gamma_{\rm L}$, which is the sum of the collisional $\nu_{\rm coll}$ and Landau damping $\gamma_{\rm L}$ contributions. The EM field corresponding to the incident laser light is enveloped at the carrier frequency $2\omega_{pe}$ and further decomposed into N, coherent, linearly polarized plane waves $\vec{E}_0 = \sum_{i=1}^{N}\vec{E}_{0,\rm i}\exp i(\vec{k}_{0,i}\cdot\vec{x} - \Omega_i t)$ having frequencies $\omega_{0,\rm i}$, wave vectors $\vec{k}_{0,\rm i} = \frac{\omega_{0,\rm i}}{c}\sqrt{1 - n_0/n_c}\hat{k}_{0,\rm i}$, and intensities $I_i = c|\vec{E}_{0,\rm i}|^2/(8\pi)$. The quantity $\Omega_i = \omega_{0,\rm i} - 2\omega_{\rm pe}$ represents the mismatch for each beam, where $\max(|\Omega_i|) \ll 2\omega_{\rm pe}$. The first term on the right-hand side of Eq. (1) is the longitudinal part of the nonlinear current, which is the origin of TPD. The term S_E is a time-random-phase Čerenkov noise

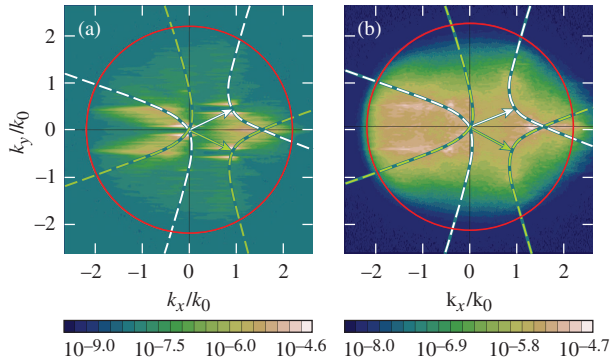

FIG. 1. The LW spectrum $\langle |E_1(k_x, k_y, k_z = 0, t)|^2 \rangle_t$ averaged over times $t = 2.4$ to 4.2 ps (a) and $t = 12.0$ to 15.0 ps (b). The two EM wave vectors $\vec{k}_{0,1}$ (green arrow), $\vec{k}_{0,2}$ (white arrow), and their polarization vectors lie in the plane shown ($k_z = 0$) (i.e., p polarization). The dashed green (white) hyperbolas correspond to the maximum single-beam homogeneous growth rate for beam 1 (2) and the red circle is the Landau cutoff $|\vec{k}|\lambda_{De} = 0.25$ (see text for parameters).

source that is implemented as described in Russell *et al.* [11] for homogeneous plasma. The results are not sensitive to the precise level.

A series of numerical calculations were carried out to solve Eq (1) on a uniform 1024 × 512×512 Cartesian grid (in the x, y, and z directions, respectively) using a 3-D generalization of the spectral method that has been described previously [10, 11]. In these calculations, the electron temperature and density scale length were held constant ($T_e = 2$ keV, $L_n = 150$ μm), while the total overlapped intensities I_{tot} ($\equiv \sum_{i=1}^{N} I_i$) was varied for various configurations of $N = 1$, 2, 4, and 6 beams of 0.351-μm-wavelength light in CH plasma ($\langle Z \rangle = 3.5$, $\langle Z^2 \rangle / \langle Z \rangle = 5.3$). For each beam configuration, the single beam intensities I_i and frequencies $\omega_{0,i}$ were taken to be equal to one another, and the beam wave vectors were distributed symmetrically to fall on the surface of a right circular cone with a 27° half-angle whose cone axis is parallel to the x direction. (see inset to **Fig. 2**). This choice of wave vectors was made because beams are distributed in well-defined cones on large laser systems such as OMEGA [12] and the NIF [13]. The simulation box length in the density-gradient direction (x) was chosen to include densities in the range of 0.19 to 0.27 n_c ($L_x = 52$ μm). The length in the two transverse dimensions was chosen to be $L_y = L_z = 26$ μm.

Two plasmon decay can be absolutely [14] or convectively unstable. [15] Absolute instability corresponds to unstable eigenmodes that grow temporally, while convective instability is limited to finite spatial amplification [16–18]. The threshold intensity for the onset of

absolute instability is found by first extracting the growth rate of the most-unstable mode, which does not saturate convectively, for a range of intensities and then finding the intensity corresponding to zero growth by extrapolation.

Figure 1(a) shows a two-dimensional slice of the LW intensity spectrum $|E_1(\vec{k},t)|^2$ in the $k_z = 0$ plane during the linear growth phase (averaged over times $t = 2.4$ to 4.2 ps) for a two-beam ($N = 2$) calculation. The EM wave vectors and electric field vectors (polarization) of the two beams lie in this plane, which is the plane of maximum growth. The overlapped intensity $I_{tot} = 6\times10^{14}$ W/cm^2 was chosen to be above the numerically determined threshold for absolute growth. In the figure, the bright "doublets" at the spectral locations centered on wave vectors $\vec{k} \approx (0.8, \pm0.4, 0)\, k_0$ and $\vec{k} \approx (0, 0, 0)$ correspond to temporally unstable (growing) decay modes that are resonant at $n_e = 0.245\, n_c$. This occurs even though each beam is individually below the threshold for absolute growth [19]. This cooperative mode of absolutely unstable TPD is analogous to the absolutely unstable modes seen in single-beam TPD, where the pump decays into one LW with $\vec{k} \sim \vec{k}_0$ and another with $\vec{k} = \pm\vec{k}_\perp$, where $|\vec{k}_\perp| \ll |\vec{k}_0|$. In the two-beam case, cooperation occurs because the long-wavelength decays near $\vec{k} \approx (0, 0, 0)$ can be shared between beams. The other local maxima in $|E_1(\vec{k},t)|^2$ located near $\vec{k} = (1.5, 0, 0)\, k_0$ and $\vec{k} = (-0.6, \pm0.4, 0)\, k_0$ are convectively saturated decays that are resonant at $n_e = 0.238\, n_c$. These correspond to convective multiple-beam common waves that have been described previously [9, 20] and the "triad" modes discussed in Refs. 8, 21, and 22. The convective gain is greatest for spectral locations where the single-beam homogeneous growth-rate curves (dashed hyperbolas in **Figs. 1**) intersect [the maxima at $\vec{k} = (-0.6, \pm0.4, 0)\, k_0$ correspond to the daughter waves that are not shared]. The maximum convective gain over all possible decay modes at the absolute threshold intensity has been computed numerically by estimating the enhancement of the saturated wave intensity above the steady-state noise level supported by S_E in Eq. (1). The behavior described above for two beams is quite generic. **Figure 2** shows $|E_1(\vec{k},t)|^2$ on the planes $k_y = 0$ and $k_z = 0$ for a four-beam calculation for the same plasma conditions as in **Fig. 1**. The beams are polarized within $x - y$ plane and predominantly in the y direction (the projections of $\vec{E}_{0,i}$ on the $y - z$ plane are parallel to each other, signified by the symbol "$\|$") as shown in the inset. The absolutely unstable modes are not restricted to a single plane. The bright spectral features near $\vec{k} = (1.0, 0, \pm0.4)\, k_0$ and $\vec{k} = (-0.2, \pm0.2, 0)\, k_0$ are again absolute multiple-beam modes. The other features in the spectrum are convectively saturated. The

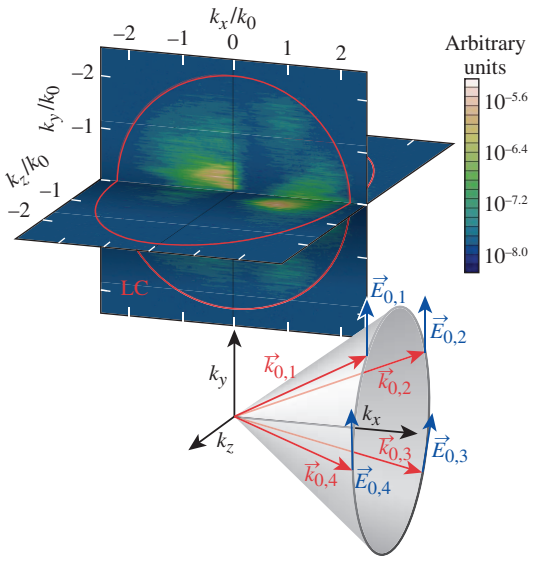

FIG. 2. Slices of the LW spectrum $\langle |E_1(\vec{k},t)|^2\rangle_t$ (averaged over times t = 1.0 to 2.0 ps) in the planes $k_y = 0$ and $k_z = 0$ for a four-beam calculation ($\|$ polarization). The beam geometry and polarization are shown in the inset.

red circles indicate the Landau cutoff.

The thresholds for cooperative absolute TPD instability for various configurations of N = 1, 2, 4, and 6 beams are summarized in **Fig. 3**. For each configuration, there are multiple possibilities for the polarization state: "p" and "s" correspond to the one- and two-beam configurations, where the polarization is in, or out of, the plane of incidence, respectively; "rad" and "tan" refer to the polarizations where the projections of the electric field vectors on $y - z$ plane are either radially or tangentially oriented with respect to the circle that forms the base of the cone containing the beam wave vectors (see inset to **Fig. 2**); the state signified as "$\|$" has been defined above. The thresholds have been quantified by normalizing the intensity of an individual beam for a given configuration $I_s = I_{tot}/N$ by the independent (single beam) absolute threshold given by Simon *et al.* [19]. For one beam ($N = 1$) at normal incidence ($\theta = 0°$), the Simon threshold [19] is recovered (as expected). [Notice that the threshold is lowered when the angle of incidence is increased to $\theta = 27°$ (triangular marker for $N = 1$ in **Fig. 3**). The effect of oblique incidence was not described in Ref. 19 and we defer a discussion of this effect to a future publication.] The cooperative nature of the instability is revealed for $N = 2$: for both s- and p-polarizations the individual (single) beam intensity at threshold $(I_s)_{thr}$ is significantly lower than the expected

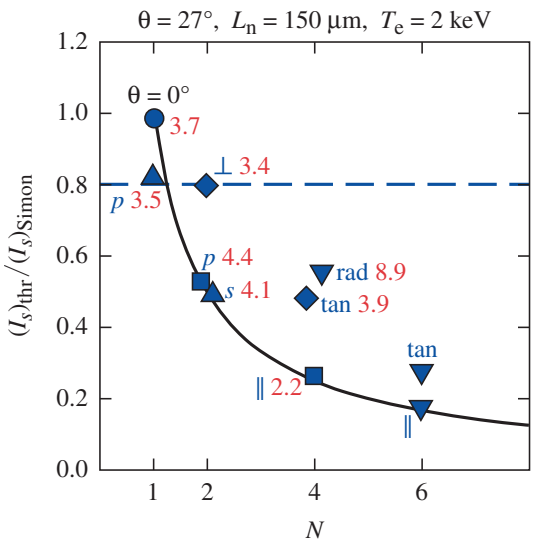

FIG. 3. Normalized single-beam threshold intensities $(I_s)_{thr}$ for absolute instability with irradiation by N beams of incidence angle $\theta_s = 27°$ (except where indicated) for various polarization states (see text). The red numbers are the maximum convective gains evaluated at the absolute threshold.

independent beam value (dashed line) — the importance of the effect increasing with the number of beams. If the daughter waves were shared exactly, the N beams would act as a single beam with N-times the single beam intensity (see the solid curve in Fig. 3). Rotating the polarizations of the two beams so as to be orthogonal ("⊥" in **Fig. 3**) eliminates the cooperation. *The overlapping beams are parametrically unstable (absolutely) even though the threshold intensity for individual beams is not exceeded.* The solid curve indicates maximum cooperation (where the collection of beams effectively act as a single beam with the combined intensity). Shown in red are the numerically estimated maximum gains of the convectively saturated common waves (cf., e.g., **Fig. 1(a)**) at an intensity corresponding to the absolute threshold. These gains are consistent with earlier work [9, 15, 23]. In most cases, this gain G is small ($G \lesssim 2\pi$) meaning that *the threshold for the cooperative absolute instability is lower than that for the convective common waves.* The regime of linear spatial amplification is therefore very restricted. Above the absolute threshold there exists a competition between the two modes of cooperative instability, which can only be addressed by a nonlinear theory.

The dominant mechanisms thought to be responsible for the nonlinear saturation of TPD (weak turbulence effects such as the Langmuir decay instability (LDI) [8, 24], profile modification [8], and the strong turbulence effects of cavitation and LW collapse [11]) are

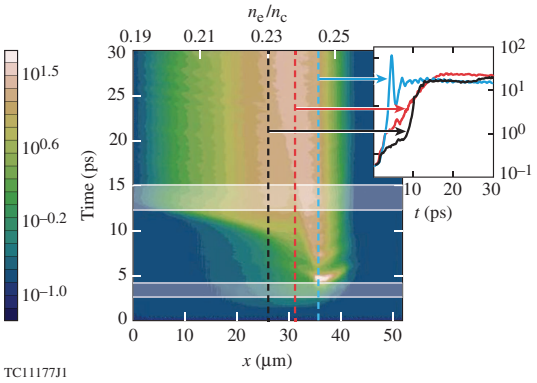

FIG. 4. The transverse averaged LW intensity $\langle|\vec{E}_1|^2\rangle_{y,z}(x,t)$ as a function of the x coordinate (initial density, upper axis) and time. The white lines mark the time windows corresponding to Fig. 1(a) and (b). The inset shows the temporal dependence of $\langle|\vec{E}_1|^2\rangle_{\perp}(x,t)$ at the locations $x = 26\,\mu$m (black dashed line) $x = 31\,\mu$m (red dashed line), and $x = 36\,\mu$m (blue dashed line).

accounted for by the substitution $\delta N \to \delta N + \delta n$ in Eq. (1), where the low-frequency plasma response δn evolves according to

$$\left[D_t^2 + 2\nu_{\rm i} \circ D_t - c_{\rm s}^2\nabla^2\right]\delta n = \frac{Z}{16\pi m_{\rm i}}\nabla^2(|\vec{E}_1|^2 + \frac{1}{4}|\vec{E}_0|^2). \tag{2}$$

Here $c_{\rm s} = (ZT_{\rm e}/m_{\rm i})^{1/2}(1 + 3T_{\rm i}/ZT_{\rm e})^{1/2}$ is the speed of ion-acoustic waves whose amplitudes damp with the rate $\nu_{\rm i}$, where $m_{\rm i}$, $T_{\rm i}$, and Z are the ion mass, temperature, and charge, respectively. The first and second terms on the right-hand side describe the low-frequency ponderomotive forces of Langmuir and electromagnetic fluctuations. Together, Eq. (1), the substitution $\delta N \to \delta N + \delta n$, and Eq. (2) constitute the extended Zakharov model of TPD, previously described in Refs. 10, 11, 22, and 25, and now generalized to three dimensions. In the context of this turbulence model where the initial ion-acoustic noise is negligible [i.e., no noise term in Eq. (2)], three regimes of cooperative TPD behavior have been identified: (1) $\tilde{I}\,[\equiv I_{\rm s}/(I_{\rm s})_{\rm thr}] < 1$ [$(I_{\rm s})_{\rm thr}$ is the single beam threshold for cooperative absolute instability (**Fig. 3**)] where the LW spectrum is dominated by large-k common waves whose intensities are amplified spatially by a gain, which is numerically determined to be small $G \lesssim 3$ to 5 (red numbers in **Fig. 3**) and consistent with the standard Rosenbluth expression [9]; (2) $\tilde{I} \gg 1$ — all unstable modes grow and saturate nonlinearly (the nonlinear development in this case has been described in terms of cavitating Langmuir turbulence and investigated in Ref. [8, 21, 22]); and (3) the intermediate regime $\tilde{I} \gtrsim 1$. The intermediate regime is of direct

relevance to spherical and planar target experiments on the Omega Laser Facility [9, 26, 27] and it displays interesting physical effects.

Figure 4 shows the nonlinear temporal evolution of the LW intensity for the two-beam p-polarized case in the intermediate regime ($\tilde{I} \gtrsim 1$) (same parameters as **Fig. 1**). The other cases shown in **Fig. 3** exhibit very similar behavior and are not shown. The transverse (y, z) average of the LW intensity $\langle|\vec{E}_1|^2\rangle_\perp(x,t)$ is shown as a function of x coordinate and time. At early times, growth is linear. The LW Fourier spectrum during this phase (indicated by the lower shaded region) is shown in **Fig. 1(a)**. The previously identified absolute and convective cooperative modes occur at different spatial locations (densities) as indicated by the blue and red dashed lines at $n_e/n_c = 0.245, 0.238$ in the figure, respectively. The blue (red) dashed vertical lines indicate the evolution of the absolute (convective) modes as a function of time (see inset). At approximately $t = 5$ ps, the absolutely unstable modes saturate nonlinearly, producing large density profile modifications and radiating large amplitude LW's. These waves propagate down the density profile [toward lower densities (smaller x)] with time, generating a region of turbulence (consistent with previous studies) whose effects can be seen in the figure. When this turbulence reaches a particular location, growth is restored to the modes that were previously convectively saturated [for $x = 26$ μm ($n_e/n_c = 0.23$), this occurs at $t \sim 10$ ps (see the black line in the inset to **Fig. 4**)]. This was verified by performing a linear analysis on the perturbed profiles. The restoration of absolute growth in a convectively unstable parametric instability (i.e., fragility of the Rosenbluth result) caused by noise or turbulence has been noted previously (cf., e.g., Ref. 28). Here, it is triggered by the nonlinearity of the absolute instability. The result is that, at late times (e.g. the upper shaded region in the figure), the LW spectrum is much broader and more intense [see **Fig. 1(b)**] than during the linear phase [**Fig. 1(a)**]. *The late-time turbulent spectrum is dominated by large-k common waves with intensities that are greatly in excess of those predicted by the linear analysis.* The effects of Langmuir wave collisional damping are to change the growth rate in the linear stages [25] and to modify the time-scale for the onset of subsequent global instability. Despite this, the same universal scenario still applies.

These results will be of fundamental importance to direct-drive ICF experiments on the NIF, where many laser beams overlap on the target (and a knowledge of TPD stability properties is essential) and are an important contribution to the understanding of cooperative parametric instabilities in general. The results obtained with this model may provide

an interpretation of experiments that infer the coexistence of large- and small-wave-number TPD LW's via half- and three-halves–harmonic emission [27, 29]. They might also explain the observation of strong TPD hot-electron production in multiple-beam OMEGA EP experiments, even though the predicted common-wave convective gains are small [9, 20].

ACKNOWLEDGMENT

This work was supported by the U.S. Department of Energy Office of Inertial Confinement Fusion under Cooperative Agreement No. DE-FC52-08NA28302, the University of Rochester, and the New York State Energy Research and Development Authority. The support of DOE does not constitute an endorsement by DOE of the views expressed in this article.

---

* jzha@lle.rochester.edu

† Also Los Alamos National Laboratory (retired).

[1] J. Nuckolls, L. Wood, A. Thiessen, and G. Zimmerman, Nature **329**, 139 (1972).

[2] J. D. Lindl, *Inertial Confinement Fusion: The Quest for Ignition and Energy Gain Using Indirect Drive* (Springer-Verlag, New York, 1998).

[3] R. P. Drake, *High-Energy-Density Physics: Fundamentals, Inertial Fusion, and Experimental Astrophysics* (Springer-Verlag, New York, 2006).

[4] D. F. DuBois, D. A. Russell, P. Y. Cheung, and M. P. Sulzer, Phys. Plasmas **8**, 791 (2001); P. Y. Cheung, M. P. Sulzer, D. F. DuBois, and D. A. Russell, *ibid.* **8**, 802 (2001).

[5] R. P. J. Town, D. K. Bradley, A. Kritcher, O. S. Jones, J. R. Rygg, R. Tommasini, M. Barrios, L. R. Benedetti, L. F. Berzak Hopkins, P. M. Celliers, T. Doppner, E. L. Dewald, D. C. Eder, J. E. Field, S. M. Glenn, N. Izumi, S. W. Haan, S. F. Khan, J. L. Kline, G. A. Kyrala, T. Ma, J. L. Milovich, J. D. Moody, S. R. Nagel, A. Pak, J. L. Peterson, H. F. Robey, J. S. Ross, R. H. H. Scott, B. K. Spears, M. J. Edwards, J. D. Kilkenny, and O. L. Landen, Phys. Plasmas **21**, 056313 (2013).

[6] P. Michel, W. Rozmus, E. A. Williams, L. Divol, R. L. Berger, S. H. Glenzer, and D. A. Callahan, Phys. Plasmas **20**, 056308 (2013).

[7] V. A. Smalyuk, D. Shvarts, R. Betti, J. A. Delettrez, D. H. Edgell, V. Y. Glebov, V. N. Goncharov, R. L. McCrory, D. D. Meyerhofer, P. B. Radha, S. P. Regan, T. C. Sangster, W. Seka, S. Skupsky, C. Stoeckl, B. Yaakobi, J. A. Frenje, C. K. Li, R. D. Petrasso, and F. H. Séguin, Phys. Rev. Lett. **100**, 185005 (2008); V. N. Goncharov, T. C. Sangster, P. B. Radha, R. Betti, T. R. Boehly, T. J. B. Collins, R. S. Craxton, J. A. Delettrez, R. Epstein, V. Yu. Glebov, S. X. Hu, I. V. Igumenschev, J. P. Knauer, S. J. Loucks, J. A. Marozas, F. J. Marshall, R. L. McCrory, P. W. McKenty, D. D. Meyerhofer, S. P. Regan, W. Seka, S. Skupsky, V. A. Smalyuk, J. M. Soures, C. Stoeckl, D. Shvarts, J. A. Frenje, R. D. Petrasso, C.-K. Li, F. Séguin, W. Manheimer, and D. G. Colombant, Phys. Plasmas **15**, 056310 (2008).

[8] H. X. Vu, D. F. DuBois, J. F. Myatt, and D. A. Russell, Phys. Plasmas **19**, 102703 (2012).

[9] D. T. Michel, A. V. Maximov, R. W. Short, S. X. Hu, J. F. Myatt, W. Seka, A. A. Solodov, B. Yaakobi, and D. H. Froula, Phys. Rev. Lett. **109**, 155007 (2012).

[10] D. F. DuBois, D. A. Russell, and H. A. Rose, Phys. Rev. Lett. **74**, 3983 (1995).

[11] D. A. Russell and D. F. DuBois, Phys. Rev. Lett. **86**, 428 (2001).

[12] T. R. Boehly, D. L. Brown, R. S. Craxton, R. L. Keck, J. P. Knauer, J. H. Kelly, T. J. Kessler, S. A. Kumpan, S. J. Loucks, S. A. Letzring, F. J. Marshall, R. L. McCrory, S. F. B. Morse, W. Seka, J. M. Soures, and C. P. Verdon, Opt. Commun. **133**, 495 (1997).

[13] E. I. Moses, R. N. Boyd, B. A. Remington, C. J. Keane, and R. Al-Ayat, Phys. Plasmas **16**, 041006 (2009); E. I. Moses, Fusion Sci. Technol. **54**, 361 (2008); W. J. Hogan, E. I. Moses, B. E. Warner, M. S. Sorem, and J. M. Soures, Nucl. Fusion **41**, 567 (2001); J. A. Paisner, E. M. Campbell, and W. J. Hogan, Fusion Technol. **26**, 755 (1994).

[14] L. V. Powers and R. L. Berger, Phys. Fluids **27**, 242 (1984).

[15] M. N. Rosenbluth, Phys. Rev. Lett. **29**, 565 (1972).

[16] R. J. Briggs, *Electron-stream interactions with plasmas*, Research Monograph no. 29 (M.I.T. Press, Cambridge, MA, 1964).

[17] A. Bers, *Linear waves and Instabilities*, Physique des Plasmas, Les Houches 1972, edited by C. De Witt and J. Peyraud (Gordon and Breach, New York, 1975).

[18] D. Pesme, in *La Fusion Thermonucléaire inertielle par laser*, Vol. 1, edited by R. Dautray and J.-P. Watteau (Eryolles, Paris, 1993) Chap. 2, p. 306.

[19] A. Simon, R. W. Short, E. A. Williams, and T. Dewandre, Phys. Fluids **26**, 3107 (1983).

[20] D. T. Michel, A. V. Maximov, R. W. Short, J. A. Delettrez, D. Edgell, S. X. Hu, I. V. Igumenshchev, J. F. Myatt, A. A. Solodov, C. Stoeckl, B. Yaakobi, and D. H. Froula, Phys. Plasmas **20**, 055703 (2013).

[21] H. X. Vu, D. F. DuBois, D. A. Russell, and J. F. Myatt, Phys. Plasmas **19**, 102708 (2012).

[22] H. X. Vu, D. F. DuBois, D. A. Russell, J. F. Myatt, and J. Zhang, Phys. Plasmas, to appear (2014).

[23] R. Yan, A. V. Maximov, and C. Ren, Phys. Plasmas **17**, 052701 (2010).

[24] D. F. DuBois and M. V. Goldman, Phys. Rev. **164**, 207 (1967).

[25] J. F. Myatt, H. X. Vu, D. F. DuBois, D. A. Russell, J. Zhang, R. W. Short, and A. V. Maximov, Phys. Plasmas **20**, 052705 (2013).

[26] C. Stoeckl, R. E. Bahr, B. Yaakobi, W. Seka, S. P. Regan, R. S. Craxton, J. A. Delettrez, R. W. Short, J. Myatt, A. V. Maximov, and H. Baldis, Phys. Rev. Lett. **90**, 235002 (2003).

[27] W. Seka, D. H. Edgell, J. F. Myatt, A. V. Maximov, R. W. Short, V. N. Goncharov, and H. A. Baldis, Phys. Plasmas **16**, 052701 (2009).

[28] D. R. Nicholson and A. N. Kaufman, Phys. Rev. Lett. **33**, 1207 (1974); G. Laval, R. Pellat, and D. Pesme, *ibid.* **36**, 192 (1976); E. A. Williams, J. R. Albritton, and M. N. Rosenbluth, Phys. Plasmas **22**, 139 (1979).

[29] W. Seka, J. F. Myatt, R. W. Short, D. H. Froula, J. Katz, V. N. Goncharov, and I. V. Igumenshchev, Phys. Rev. Lett. **112**, 145001 (2014).

*